Available online at www.eccomasproceedia.org
Eccomas Proceedia COMPDYN (2017) 4584-4594

ECCOMAS
Proceedia

COMPDYN 2017
6th ECCOMAS Thematic Conference on
Computational Methods in Structural Dynamics and Earthquake Engineering
M. Papadrakakis, M. Fragiadakis (eds.)
Rhodes Island, Greece, 15–17 June 2017

SMALL-STRAIN STIFFNESS AND DAMPING OF LOESS IN CHINA

Binghui. Song[1,2], Angelos. Tsinaris[2], Anastasios. Anastasiadis[2], Kyriazis. Pitilakis[2], and Wenwu. Chen[1]

[1] Key Laboratory of Mechanics on Disaster and Environment in Western China, the Ministry of Education of China and College of Civil Engineering and Mechanics, Lanzhou University, Lanzhou, 730000 P.R. China
e-mail: songbh09@gmail.address, sungp@lzu.edu.cn

[2] Department of Civil Engineering, Aristotle University of Thessaloniki, P.O.B. 424, Thessaloniki, 54124 Greece
e-mail: tsinaris@civil.auth.gr, anas@civil.auth.gr, kpitilak@civil.auth.gr

Keywords: Loess, Small-Strain Stiffness, Damping, Resonant Column Test, Down-hole Test.

Abstract. *Loess Plateau of China is one of the most representative geomorphologic regions for loess around the world due to the deep covering layer and wide distribution area. Many catastrophic disasters induced by earthquake had been identified in this area. This study examined systematically the small-strain stiffness and damping of loess in Lanzhou, Northwest of China, through the laboratory resonant column (RC) test method and the field down-hole test method. On the basis of the analyses of test results, it was found that the small-strain shear modulus G_0 of loess was more sensitive to water content than the small-strain damping D_{min}. A linear relationship between log(G_0) and log(σ'_m) was observed for loess, while the corresponding slope in log-log coordinates decreased with water content increasing. Similarly, log(D_{min}) decreased linearly with log(σ'_m) as well. G_0 of undisturbed loess was much higher than reconstituted ones at low water content and this difference could be negligible for saturated loess. The similar phenomenon was observed for D_{min} too. The pattern of correlation between G_0 and σ'_m for loess accorded well with the findings in literature but in the present study, higher values of G_0 could be expected, which may be ascribed to the different device used. In comparison with the down-hole test results, there was a good agreement between RC results and laboratory results for G_0 of loess. Finally, the correlations between G/G_0 and $\gamma/\gamma_{0.85}$ could be normalized perfectly for Lanzhou loess, irrespective of water content and confining pressure.*

Peer-review under responsibility of the organizing committee of COMPDYN 2017.
doi: 10.7712/120117.5745.16959

1 INTRODUCTION

China loess is a kind of aeolian deposited loess, covering more than 6.3% of the country's land area (named loess plateau) distributed mainly at the northwest regions of China as overlaying soil [1, 2]. The thickest loess profile reported in Lanzhou is more than 400m [3], which is one of the most representative loess profiles in the world.

Loess Plateau was an earthquake-prone area where tectonic movements were very active and throughout history several catastrophic disasters caused by earthquakes had been identified and documented fully [4, 5]. Studies on the dynamic properties of loess were very essential and significant to the mission of earthquake protection and mitigation in this region. Several recent researches on the stress-strain properties during cyclic loading of loess were conducted in the laboratory by using conventional cyclic triaxial testing [6, 7, 8], while the cyclic strains investigated in these studies were large ($>10^{-2}$%) due to the lack of sensitive LVDT with high precision. Actually, studies on the stress-strain properties of loess during cyclic loading at small strain levels, especially considering the effect of various factors, e.g. water content, confining pressure and soil structure, are rather limited [9, 10]. In this research work, a comprehensive set of resonant column tests were conducted to evaluate the stress-strain properties of loess under relatively fast cyclic loading conditions from small to medium shear strains (10^{-5}%$<\gamma<10^{-2}$%), in order to improve the research level of the dynamic properties of loess.

2 TEST PROGRAM

2.1 Testing material

The studied loess specimens were collected from a geotechnical borehole in the National New Area of Lanzhou, Northwest of China. The representative soil profile of the studied site is shown in Figure 1 with the corresponding SPT blows and the shear wave velocity V_s obtained from down-hole measurements included as well.

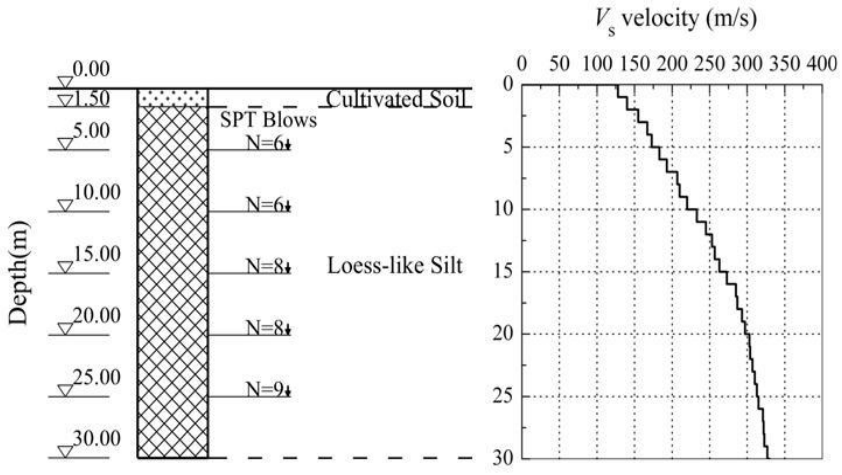

Figure 1: Loess profile with in situ test results.

As shown in Figure 1, apart from limited thickness of the top cultivated soil layer (about 1.5m), loess-like silt which is commonly designated as Q_4 loess [11] in China based on the age of deposition, comprises the major part of the investigated soil strata. The variation of SPT blows for loess ranges from 6 to 9 within the top 25m thickness, which can be attributed

to the metastable structure of loess with high void ratio. In addition, shear wave velocity of loess obtained from down-hole measurements increases monotonically with depth indicating relatively homogeneous soil strata with depth. A series of undisturbed loess specimens with different burial depth were collected from the borehole and shipped carefully to the laboratory for subsequent tests. Table 1 presents the basic physical properties of loess.

Table 1: Physical properties of loess in natural condition.

Sample	Depth (m)	Water content W (%)	Total density ρ_t (g/cm^3)	Void ratio e	Specific Gravity γ_s	LL (%)	PL (%)
LZL-4	4	14.33	1.50	1.058	2.70	24.31	16.62
LZL-6	6	13.42	1.53	1.002	2.70	24.80	16.71
LZL-8	8	11.54	1.49	1.029	2.71	24.72	16.63
LZL-10	10	14.21	1.55	0.997	2.71	24.52	17.12
LZL-12	12	16.93	1.54	1.058	2.71	25.41	17.82
LZL-13	13	16.11	1.56	1.017	2.71	25.72	18.40

Based on the physical properties (Table 1) and the particle size distribution of loess shown in Figure 2, Lanzhou loess is classified as CL silt loam according to the unified soil classification system (USCS).

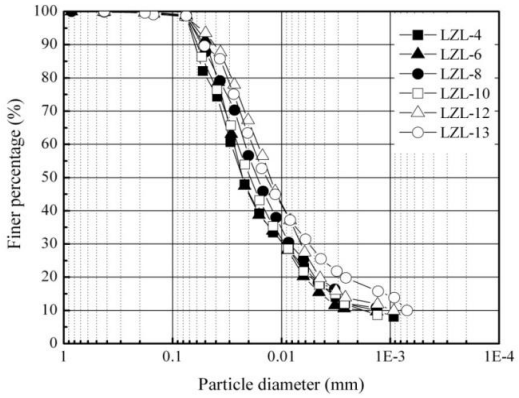

Figure 2: Particle composition characteristics of loess.

In order to investigate the effect of water content on the dynamic properties of loess, wetting and drying method [12, 13] were adopted to prepare loess specimens with various water contents. Saturated specimens were prepared under the standard procedure of saturation by using the back-pressure method. Following the same principles, reconstituted specimens having the same water content and dry density with undisturbed specimen were prepared following the standard compaction method [14]. In total, eight groups of loess specimens were prepared for RC test with their characteristics shown in Table 2.

Table 2: Physical properties of loess in natural condition.

Sample	Depth (m)	Current moisture (%)	Current saturation (%)
LZL-4-U(1)	4	24.41	59.95
LZL-6-U	6	6.83	18.90
LZL-6-R(2)	6	6.52	18.15
LZL-8-U	8	22.52	56.08
LZL-10-U	10	13.69	37.56
LZL-12-U	12	17.11	43.71
LZL-13-U	13	33.41	84.00
LZL-13-R	13	34.58	86.44

Note: (1) U means undisturbed specimen; (2) R represents reconstituted specimen; Current moisture (%) is the water content of loess measured after wetting or drying process

A resonant column device of free-fixed end designed by Drenvich [15] and manufactured by Soil Dynamics Instruments (Soil Dynamics Instruments, Inc), capable of longitudinal and torsional dynamic loading was used. The dimension of loess specimen was 140mm in height and 70mm in diameter. The whole experimental procedure and the analysis of the RC test results were performed according to the ASTM 4015-92 specification [16].

3 EXPERIMENTAL RESULTS AND DISCUSSION

3.1 Small-strain shear modulus G_o

(a) Effect of water content

Figure 3 presents the influence of water content against small-strain shear modulus G_0 for undisturbed Lanzhou loess obtained from the present testing program together with results stemming from literature [17].

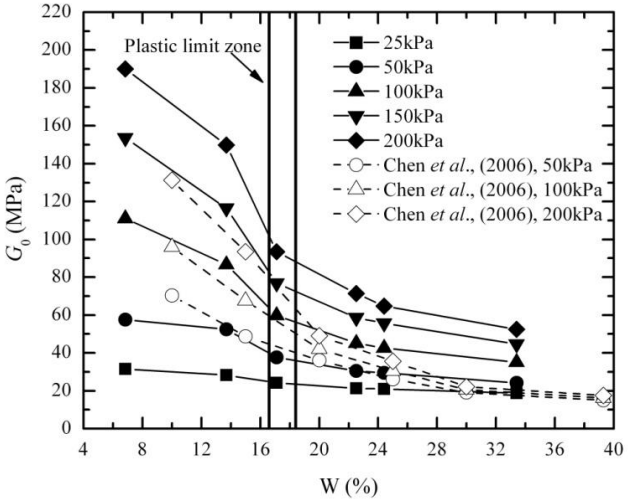

Figure 3: Relationships between G_0 and W for loess.

As shown in Figure 3, under the same confining pressure, the initial shear modulus G_0 of loess decreases continuously with water content. It is interesting to notice that when water content approaches the plastic limit, there is a dramatic decrease of G_0, especially for the cases of high confining pressure (≥100kPa). According to [17], the correlations between G_0

and water content for loess measured in cyclic triaxial test, coincides well with the trends of G_0 with water content in the present study. However, due to the limitations of the apparatus, the values of G_0 reported in [17] under the same confining pressure, are a bit lower than the corresponding ones of our study, especially for high confining pressures and water contents.

(b) Effect of confining pressure

A power function initially proposed in [18] has been widely used to describe the quantitative relationship between the small-strain shear modulus G_0 and effective mean confining stress σ'_m:

$$\frac{G_o}{P_r} = \frac{A}{F(e)} * \left(\frac{\sigma_m^{'}}{P_r}\right)^m \tag{1}$$

where, P_r is reference pressure and can be set as 1kPa; A is a dimensionless material constant with respect to soil types; $F(e)$ is a function of void ratio e and commonly $F(e)=(1+e)/(2.973-e)^2$ for most kinds of soil; m is the exponent representing the effect of effective mean confining stress σ'_m on G_0.

Figure 4 shows the effect of the mean effective confining pressure σ'_m on the small-strain shear modulus G_0 of the tested undisturbed Lanzhou loess specimens in this work. The correlations between G_0 and σ'_m are fitted by using Equation (1) and the corresponding fitting results are shown in Figure 4 and Table 3.

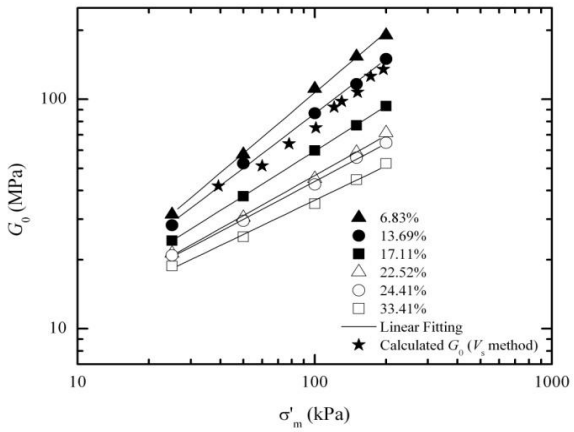

Figure 4: Relationships between G_0 and σ'_m for loess.

Table 3: Fitting parameters of Hardin equation for Lanzhou loess.

Water content (%)	A	m	Correlation coefficient R^2	Shear strain amplitude (%)
6.83	973.48	0.876	0.999	3.9×10^{-5}-1.2×10^{-4}
13.69	1183.96	0.788	0.999	5.6×10^{-5}-2.2×10^{-4}
17.11	1535.60	0.650	0.999	9.9×10^{-5}-3.0×10^{-4}
22.52	1662.83	0.579	0.998	1.3×10^{-4}-3.0×10^{-4}
24.41	1816.97	0.547	0.999	1.3×10^{-4}-3.0×10^{-4}
33.41	1911.43	0.495	0.998	1.2×10^{-4}-3.0×10^{-4}

Note: Shear strain amplitude (%) where G_0 and D_{min} are defined in this study and lower values correspond to higher confinement stress.

As shown in Figure 4, it is observed that there is a clear linear increase of G_0 with σ'_m in double logarithm coordinates, and the inclination decreases with the water content. The values of the G_0 calculated using the shear wave velocity V_s (Figure 1) which is measured through down-hole method are also presented in Figure 4. The comparisons with our laboratory results are quite good for natural water content W around 14%.

The variations of the exponent m and dimensionless constant A with water content are shown in Figure 5. The relevant empirical correlations are formulated as follows:

$$m = 1.813 * W^{-0.361} \tag{2}$$

$$A = 398.553 * W^{0.457} \tag{3}$$

where, W is the water content of loess.

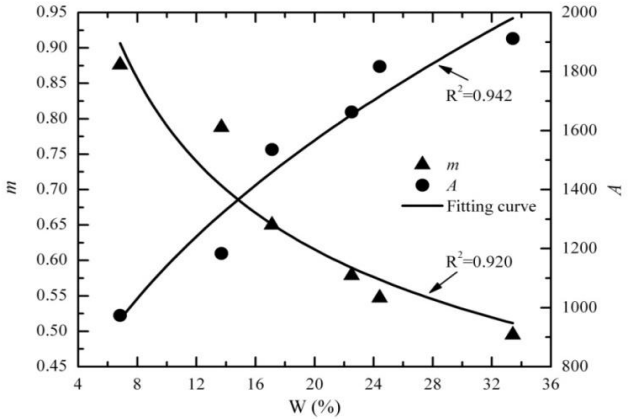

Figure 5: Correlations between fitting parameters (m and A) and water content.

(c) Effect of structure strength

The results of small-strain stiffness G_0 for undisturbed and reconstituted loess are compared in Figure 6. As illustrated, when loess is a little dry, e.g. LZL-6-U/R specimens, the difference of G_0 between undisturbed and reconstituted specimens is big, while the values of G_0 between the undisturbed and reconstituted specimen are very close in saturated state.

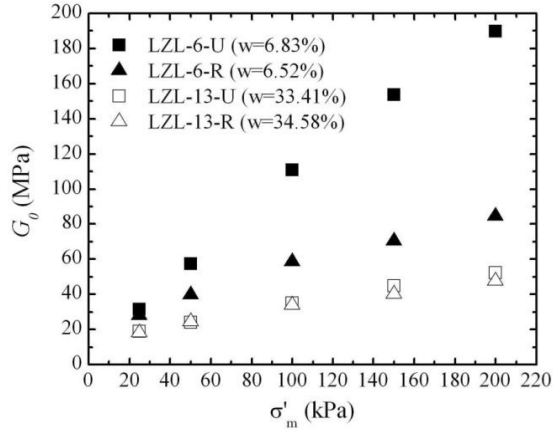

Figure 6: Comparison of G_0 values between undisturbed and reconstituted loess.

3.2 Small-strain damping D_{min}

(a) Effect of water content

Figure 7 depicts the variations of D_{min} of loess with water content under different confining pressures. As shown, with the increase of water content, D_{min} of loess decreases firstly and then tends to increase when loess is fully saturated. Regarding the limited range of D_{min}, it can be concluded that the effect of water content on D_{min} of loess is insignificant.

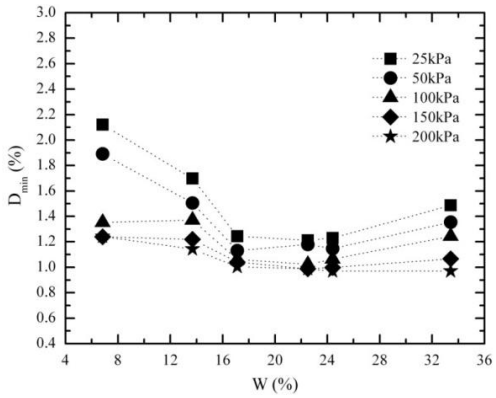

Figure 7: Effect of water content on the small-strain damping ratio D_{min}.

(b) Effect of confining pressure

The general trends of the effect of the mean effective confining stress σ'_m on the small-strain damping ratio D_{min} of Lanzhou loess are illustrated in Figure 8, where the representative experimental results of D_{min} for sand and cohesive soils [19, 20, 21] are included in the same figure as well. Table 5 summarizes the fitting results of the relationships between D_{min} and σ'_m.

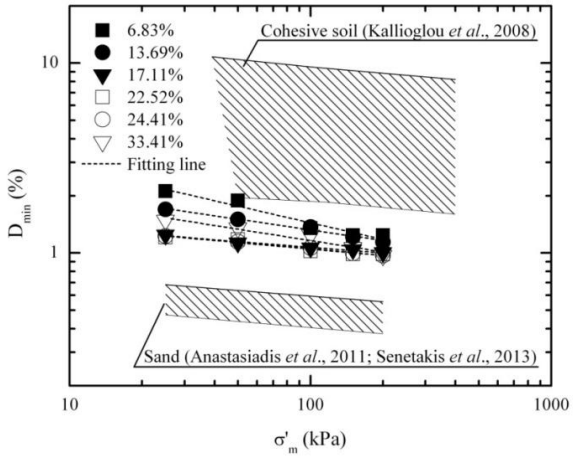

Figure 8: Effect of mean effective confining stress σ'_m on the small-strain damping ratio D_{min}.

As shown in Figure 8, it can be observed that D_{min} of loess decreases linearly as confining stress increases in double logarithm coordinates. In comparison to the data of D_{min} of sand published in [20, 21], loess possesses higher values of D_{min} under the same confining pressure. However, the data of D_{min} of loess are much lower than that of cohesive soils with

higher PI published in [19]. From a qualitative point of view, it appears that the small-strain damping ratio D_{min} of soil has the trend to increase with plasticity index, which is consistent with the findings presented in [22].

(c) Effect of structure strength

The effect of structure strength on D_{min} of loess is illustrated in Figure 9. It can be seen from Figure 9 that D_{min} of undisturbed loess is higher than for remolded loess under the same confining pressure, which may result from the alternation of soil fabric [23]. However, the effect of structure strength of loess on D_{min} is limited in view of the small variation of D_{min} in Figure 9.

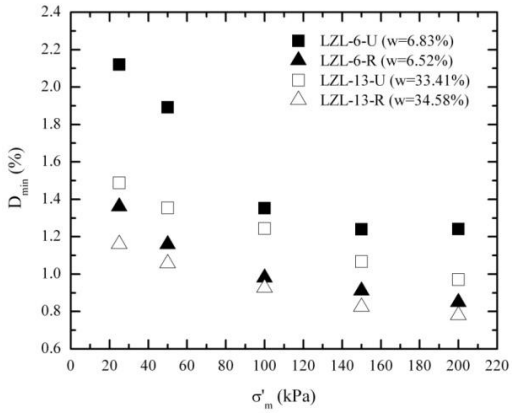

Figure 9: The small-strain damping ratio D_{min} of undisturbed and reconstituted loess specimens.

3.3 G/G_o-γ curves

The relationship between normalized shear modulus G/G_0 and shear strain γ characterized the behavior of soil stiffness degradation [24]. Figure 10 depicts the variation of G/G_0 with γ determined for intact loess under different confining pressures. As shown, the normalized shear modulus G/G_0 degrades continuously with the increment of shear strain, and the degradation curves tend to move up and to the right as confining pressure increases. Although the data points of G/G_0 vs. γ curves between different confining pressures are scattered, most of them fall into a relative narrow band corresponding to the curves with plasticity indexes of 0 and 30, respectively [25].

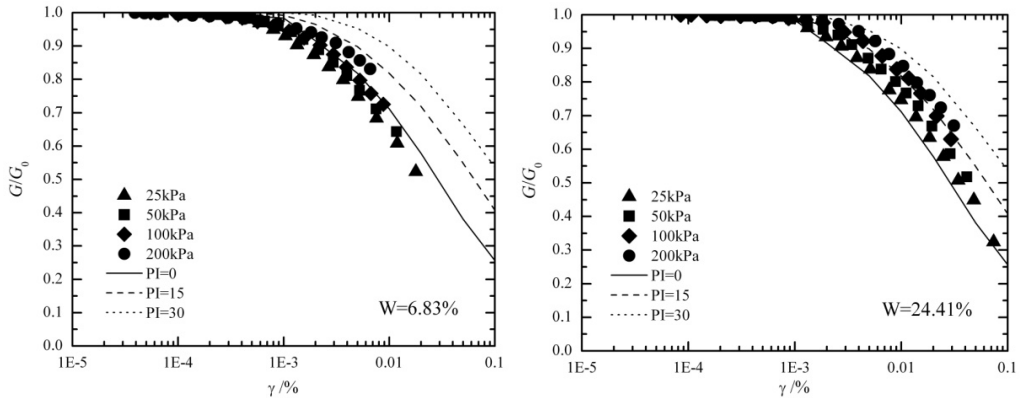

Figure 10: Effect of shear strain amplitude (γ) and confinement on the normalized shear modulus (G/G_0) of loess specimens with different water content (in the same figure the empirical curves for cohesive soil are also shown [25]).

On the basis of a summarization of previous researches, volumetric threshold shear strain, γ_v, was proposed to define significant changes in the cyclic soil behaviour [26]. After that, γ_v was adopted as a reference shear strain to depict the normalization characteristics of G/G_0 vs. γ curves [27, 28] based on the conventional stress-strain hyperbolic model given in [24] shown as Equation (4):

$$\frac{G}{G_o} = \frac{1}{\left[1+(\frac{\gamma}{\gamma_v})^a\right]} \tag{4}$$

where, G is the secant shear modulus of soil; G_0 is the initial shear modulus; a is a fitting parameter; γ is shear strain; γ_v is reference shear strain.

Considering the structure strength of undisturbed loess, $\gamma_{0.85}$ was adopted in this study to investigate the normalization characteristics of relationships between G/G_0 and γ for Lanzhou loess. The modified relationships between G/G_0 and $\gamma/\gamma_{0.85}$ were presented in Figure 11 with the corresponding fitting curve included in the same figure as well. As indicated in Figure 11, there is almost a perfect coincidence for all the curves of G/G_0 vs. $\gamma/\gamma_{0.85}$ for Lanzhou loess, irrespective of water content and confining pressure. The fitting results shown in Figure 11 verified the feasibility of the empirical model (Equation (4)) to describe the normalized relationship between G/G_0 and $\gamma/\gamma_{0.85}$ for Lanzhou loess.

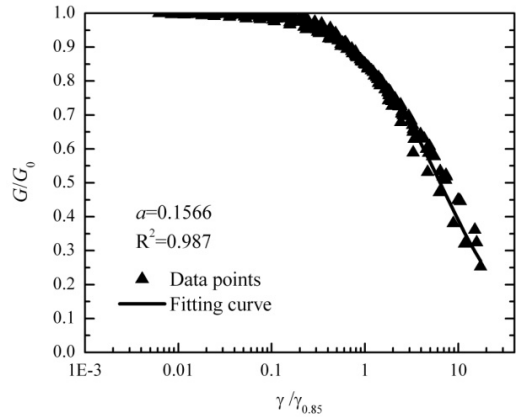

Figure 11: Normalized relationship between G/G_0 and $\gamma/\gamma_{0.85}$ for Lanzhou loess.

4 CONCLUSIONS

- Small-strain shear modulus G_0 of loess was more sensitive to water content than the small-strain damping D_{min}.
- $\log(G_0)$ increased and $\log(D_{min})$ decreased linearly with $\log(\sigma'_m)$.
- Small-strain shear modulus G_0 of undisturbed loess was much higher than reconstituted ones at low water content, and this difference could be negligible for saturated loess. The similar case was observed for D_{min} as well.
- The correlations between G/G_0 and $\gamma/\gamma_{0.85}$ could be normalized perfectly for Lanzhou loess, irrespective of water content and confining pressure.

REFERENCES

[1] Lin Z.G, Liang W.M, Distribution and engineering properties of loess and loesslike soils in China. Schematic map of engineering geological zoning. *Bulletin of the International Association of Engineering Geology*, **21**: 112-117, 1980.

[2] Lin Z.G, Liang W.M, Engineering properties and zoning of loess and loess-like soils in China. *Canadian Geotechnical Journal*, **19**(1): 76-91, 1982.

[3] Chen F.H, Li J.J, Zhang W.X, Loess stratigraphy of the Lanzhou profile and its comparison with deep-sea sediment and ice core record. *GeoJournal*, **24**(2): 201-209, 1991.

[4] Luo W.B, Seismic problems of cave dwellings on China's loess Plateau. *Tunnelling and Underground Space Technology*, **2**(2): 203-208, 1987.

[5] Zhang Z, Wang L, Geological Disasters in loess areas during the 1920 Haiyuan earthquake, China. *GeoJournal*, **36**(2): 269-274, 1995.

[6] Wang J, Yuan Z.X, Li L, Study on liquefaction of loess site. *Proceedings of the 4th international conference on earthquake geotechnical engineering*, Thessaloniki, Greece, 2007.

[7] Yuan Z.X, Wang L.M, Collapsibility and seismic settlement of loess. *Engineering Geology*, **105**: 119-123, 2009.

[8] Wang L.M, Wu Z.J, Xia K, Study on the effect of loess sites on seismic ground motion and its application in seismic design. *Proceedings of the 6th International Conference on Earthquake Geotechnical Engineering*, Christchurch, New Zealand, 2015.

[9] Wang Q, Sun J, Wang L.M, Chen X,. Review and discussion on seismic subsidence of loess. *Earthquake Research in China*, **27**(4): 479-489, 2013.

[10] Tian W, Wang L, Sun J, Xu S, Liu K, Sun Y, Progress and possible breakthroughs in research into the dynamic deformation of loess. *Journal of Lanzhou University (Natural Sciences)*, **50**(5): 645-652, 2014. (In Chinese with English Abstract)

[11] Liu D.S, Zhang Z.H, Chinese loess. *Acta Geologica Sinica*, **42**(1): 1-14, 1962. (In Chinese with English Abstract)

[12] Haeri S.M, Zamani A, Garakani A.A, Collapse potential and permeability of undisturbed and remolded loessial soil samples. *Unsaturated soils: Research and applications*, Springer, New York: 301-308, 2012.

[13] Wen B.P, Yan Y.J, Influence of structure on shear characteristics of the unsaturated loess in Lanzhou, China. *Engineering Geology*, **168**: 46-58, 2014.

[14] Ladd R.S, Preparing test specimens using undercompaction. *Geotechnical Testing Journal*, **1**(1): 16-23, 1978.

[15] Drnevich V.P, Hardin B.O, Shippy D.J, Modulus and damping of soils by the resonant-column method. *Dynamic Geotechnical Testing, ASTM STP 654, American Society for Testing and Materials*: 91-125, 1978.

[16] ASTM, Standard test methods for modulus and damping of soils by the resonant column method: D4015-92. Annual Book of ASTM Standards, ASTM International, 1992.

[17] Chen C, He J, Gao P, Dynamic deformation characteristics of intact loess under different water content. *Journal of Xi'an University of Technology*, **22**(4): 390-394, 2006. (In Chinese with English Abstract)

[18] Hardin B.O, Richart F.E, Elastic wave velocities in granular soils. *Journal of Soil Mechanics and Foundations Division*, **89**(SM1): 33-65, 1963.

[19] Kallioglou P, Tika T, Pitilakis K, Shear modulus and damping ratio of cohesive soils. *Journal of Earthquake Engineering*, **12**(6): 879-913, 2008.

[20] Anastasiadis A, Senetakis K, and Pitilakis K, Small-strain shear modulus and damping ratio of sand-rubber and gravel-rubber mixtures. *Geotechnical and Geological Engineering*, **30**(2): 363-382, 2011.

[21] Senetakis K, Anastasiadis A, Pitilakis K, Coop M.R, The dynamics of a pumice granular soil in dry state under isotropic resonant column testing. *Soil Dynamics and Earthquake Engineering*, **45**: 70-79, 2013.

[22] Lanzo G, Vucetic M, Effect of soil plasticity on damping ratio at small cyclic strains. *Soils and Foundations*, **39**(4): 131-141, 1999.

[23] Ashmawy A.K, Salgado R, Guha S, Drnevich V.P, Soil damping and its use in dynamic analyses. *International Conferences on Recent Advances in Geotechnical Earthquake Engineering and Soil Dynamics*, Paper 9, 1995.

[24] Hardin B.O, Drnevich, V.P, Shear modulus and damping in soil: design equations and curves. *Journal of the Soil mechanics and Foundation Engineering Division*, **98**(7): 667-692, 1972.

[25] Vucetic M, Dobry R, Effect of Soil Plasticity on Cyclic Response. *Journal of Geotechnical Engineering*, **117**(1): 89-107, 1991.

[26] Vucetic M, Cyclic threshold shear strain in soils. *Journal of Geotechnical Engineering*, **120**(12): 2208-2228, 1994.

[27] Santos J.A, Correia A.G, Shear modulus of soils under cyclic loading at small and medium strain level. *12th World Conference on Earthquake Engineering*, paper ID 0530. Auckland, New Zealand, 2000.

[28] Correia A.G, Santos J.A, Barros J.M.C, Niyama S, An Approach to Predict Shear Modulus of Soils in the Range of 10^{-6} to 10^{-2} Strain Levels. *International Conference on Recent Advances in Geotechnical Earthquake Engineering and Soil Dynamics*. San Diego, California, Missouri University of Science and Technology. Paper 18, 2001.